Molecular structure at the surface of a polar model liquid

1996 J. Phys.: Condens. Matter 8 3767

(http://iopscience.iop.org/0953-8984/8/21/005)

J. Phys.: Condens. Matter **8** (1996) 3767–3784. Printed in the UK

Molecular structure at the surface of a polar model liquid

Johannes Dietter and Harald Morgner

Institut für Experimentalphysik, Naturwissentschaftliche Fakultät, Universität Witten/Herdecke, Stockumer Strasse 10, D-58448 Witten, Germany

Received 25 August 1995, in final form 2 January 1996

Abstract. We have simulated a liquid layer consisting of quasi-Stockmayer molecules with the molecular dynamics method. Graphical illustration of the ensemble shows that the molecules form chains. The calculation of the chain size distribution for the bulk part and for the surface of the layer shows that in the bulk part of the liquid longer chains are more likely to occur. We reason that this is due to the higher mobility of the molecules in the surface region which lowers the probability of bond formation.

In addition to this we have analysed the topological correlation between chains. To do so a distance between chains has been defined to obtain a criterion for whether two chains are neighbours or not. We have examined the angles between those molecules of two neighbouring chains which are closest or between those with the lowest pair energy. It seems that there is a slight preference that the two closest molecules of the neighbouring chains align their dipoles. If the chain sizes of the two participating chains exceed three an increase in the probability that the two closest molecules antialign their dipoles can also be observed. A rise in the dipole moment intensifies this behaviour. Lowering the moment of inertia yields a decrease in the probability to antialign the neighbouring dipoles. A possible reason is the loss of stability of the antiparallel arrangement due to an increased amplitude of the rotational vibration caused by the smaller moment of inertia. However, the parallel arrangement is still a preferred orientation between the correlated dipoles.

1. Introduction

Computer simulation methods have been used to examine the liquid–vapour interface by simulating a liquid layer. The systems used were model liquids [1–4, 6] as well as systems for real liquids [7–9]. The model liquids consisted of Lennard-Jones atoms [1] or of site-site Lennard-Jones diatomics with [2] and without [3] quadrupole moment. Eggebrecht *et al* [4] used a Stockmayer fluid and compared the results of their simulation to their previous theoretical work [5]. Within this work they applied integral equation and perturbation theories to the liquid. A reaction field method for a liquid layer was developed in [6]. In [1–3] and [6] the authors focused on number density profile, orientation-density profile and surface tension. In addition to this Eggebrecht *et al* [4] investigated the dynamical behaviour of particles in the surface in contrast to the bulk.

Matsumoto and Kataoka performed MD simulations of water [7] and methanol [8]. They studied structural and thermodynamic properties which are sensitive to the presence of the two surfaces. Amaral and Cabral [9] simulated a liquid layer of methylchloride with the Monte Carlo method. They specifically examined the dependence of the calculated quantities on the ensemble size by treating systems with different numbers of molecules.

The study of structure formation seems to be somehow concentrated on bulk systems. In water the analysis of rings formed by single water molecules showed some insight into

0953-8984/96/213767+18$19.50

the structure of the liquid [10, 11]. For methanol a long winding chain was found to be the basic structure [12, 13]. Dynamical aspects of hydrogen bonding in methanol are discussed in [14]. The authors also calculated the distribution of chain sizes in methanol. Chains are also subject to discussion in the case of liquid formamide. Experimental results obtained by ESCA (XPS) [15] and NMR [16] were explained with the assumption of linear chains in the liquid. Jorgensen and Swenson [17] performed MC simulation of liquid formamide and proposed that formamide molecules form chains with parallel alignment of dipoles, and that neighbouring chains are formed by molecules with opposite direction of dipoles to the first one. More recently Puhovsky *et al* [18] simulated formamide with the MD method and found their data more compatible with a complicated H-bond network. The MD simulation of formamide by Schoester *et al* [19] revealed a mixture of ring and chain conformations.

The behaviour of chainlike molecules in a spatially inhomogeneous situation has been studied for liquids composed of polymers. Bitsanis *et al* simulated a polymer confined between two solid surfaces [20, 21]. In [22] the liquid layer was confined between two solid surfaces as well, but in a semi-droplet configuration. That means that it was of infinite extent in one of the directions parallel to the solid surfaces and finite in the other direction, exposing a liquid–vacuum interface.

In polymers the chains exist per definition whereas in our system simple quasi-Stockmayer molecules form chains similar to those found in methanol [12–14]. Our aim was to examine the formation of chains in a spatially inhomogeneous system such as a liquid layer. First we investigated the nature of the bonding between two molecules to make sure that we could apply the usual bonding criterion [14]. With this information we calculated the chain size distribution for bulk and surface respectively. To take the structural analysis one step further we looked for an orientational correlation between chains which yields a hierarchy of structure elements to describe the topology of the liquid. This latter examination was performed without distinguishing between bulk or surface behaviour.

2. Simulation technique

The model molecule is the same as in [6]. The model molecule is a so called quasi-Stockmayer molecule which consists of three sites linearly and equidistantly arranged. The central site is a Lennard-Jones centre and has no charge. The outer sites carry equal and opposite charges and have equal masses. The central site has no mass (only in subsection 3.4 do we show the results of a simulation with a different mass distribution). The molecule is rigid without any internal degrees of freedom. A real Stockmayer molecule consists of a point dipole together with a Lennard-Jones centre and an arbitrarily assigned moment of inertia. That means that the main difference to our quasi-Stockmayer molecule is the treatment of the Coulomb interaction. In [6] it was chosen in order to mimic in a simple fashion some features of the formamide molecule. The feature common to the quasi-Stockmayer molecule and the formamide molecule is that the molecular dipole is directed along the molecular axis. This is exact for the quasi-Stockmayer molecule and approximately valid for the formamide molecule. The most important difference is the arrangement of the Lennard-Jones centres. The quasi-Stockmayer molecule has one Lennard-Jones centre so the corresponding interaction is isotropic. The models for the formamide molecule posses three [17] or even six [19] Lennard-Jones centres which means that the corresponding interaction is highly anisotropic. The exact parameters of the quasi-Stockmayer molecule are given in table 1 along with other simulation details.

Our program is based on the MD program MDMPOL [23] from the CCCP5 library which uses the Verlet algorithm with the quaternion technique for numerical integration

Table 1.

e = elemental charge	
k = Boltzmann constant	
u = atomic mass unit	
Charge distance within a molecule	$l = 2.142$ Å
Charge	$q = \pm 0.136\,09\ e$
Site masses	$m = 20$ u
Lennard-Jones parameter	$\varepsilon/k = 120$ K, $\sigma = 3.4$ Å
Temperature	$T = 130$ K
Box length (x, y plane)	$L = 23.07$ Å
Box length in z direction	$L_z = 3L$
Potential cutoff	$r_c = L/2$
Run length	nstep = 80 000
Time step	dt = 1 fs
Energy conservation	$\Delta E/E \leqslant 0.01\%$
Number of molecules	$n = 256$

of equation of motions. Long-range interactions were taken into account via the Ewald summation method. The system was equilibrated with the same box length for all three directions for 30 ps. During this period velocities were rescaled every second time step to achieve the desired temperature. Following this the box size was increased in the z-direction by a factor of three. This results in the simulation of a system which is extended to infinity in the x and y directions via periodic boundary conditions, but due to the extension in the z direction the distance to the next periodic replica in the z direction is large enough for the development of free surfaces on both sides of the liquid layer. This method has already been used by Matsumoto and Kataoka [7, 8] and Alejandre *et al* [24]. The increased box length in the z direction has to be taken in to account if one calculates the Ewald sum. In particular, the number of allowed k vectors in the z direction has to be increased according to the increase of the box length in the z direction. To be commensurate with the modified cell geometry the number of allowed k vectors in the z direction was increased by a factor of three. This procedure was not explicitly stated by Matsumoto and Kataoka [7, 8] but it was by Alejandre *et al* [24]. After the extension of the box in the z direction another equilibration period of 20 ps was followed by velocity rescaling every 10th time step to establish a stable surface. After this the temperature was free to fluctuate and data sampling began over a period of 80 ps. No external field was applied to maintain a stable surface.

3. Results and discussion

3.1. One- and two-particle distributions

Since our main interest is the exploration of the chain formation we first have to clarify the bonding between two molecules. One possibility of defining a bonding criterion [14] is connected with the distribution of the pair energies (see figure 1). This distribution shows a very high maximum around zero pair energy (only the rise to this maximum is visible in figure 1) which results from two arbitrarily chosen molecules and a smaller one caused by the bonded molecules. The pair energy at the minimum is a natural choice as a limit pair energy: molecules are defined as bonded if their pair energy is below this limit and unbonded if above. We have used time averaged pair energies, the averaging interval being

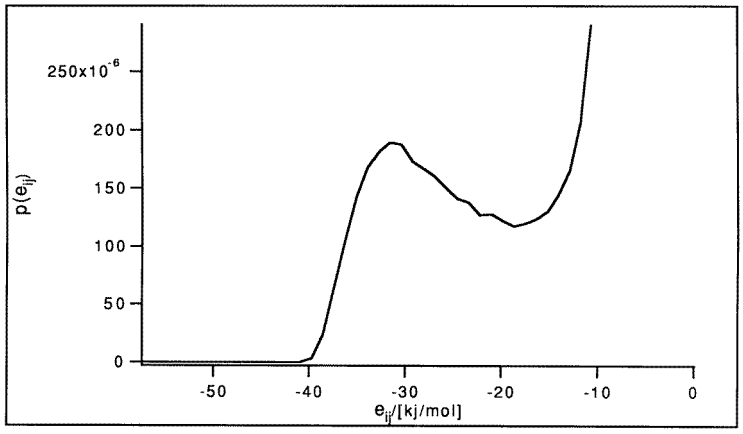

Figure 1. The distribution of the pair energy. The distribution is normalized to unity.

of the order of the intermolecular vibrations:

$$\overline{\varepsilon_{ij}}(t) = \frac{1}{\Delta}\int_{t-\Delta/2}^{t+\Delta/2} \varepsilon_{ij}(t')\,\mathrm{d}t'.$$

This is analogous to the concept of the v-structure (vibrational averaged structure) for water [25]. We have calculated the autocorrelation function of the projection of velocities on the molecular axis to obtain a rough measure for the averaging time Δ (figure 2). We took 0.3 ps as a reasonable value.

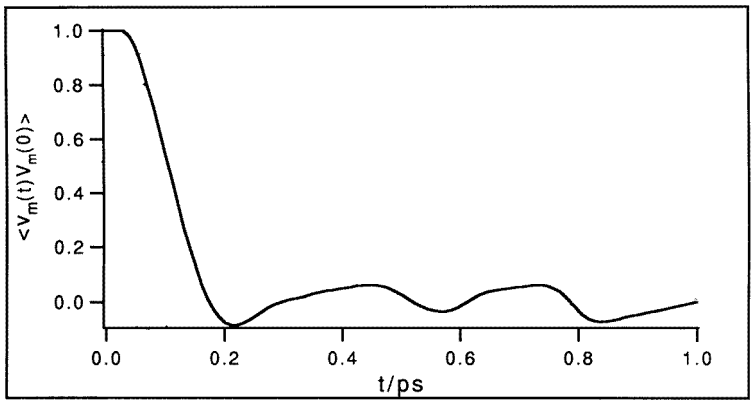

Figure 2. The autocorrelation function of the projection of the centre of mass velocity onto the molecular axis.

The distribution of bond lifetimes is shown in figure 3. The average lifetime is defined as

$$T = \int_0^\infty t_b\, p(t_b)\,\mathrm{d}t_b$$

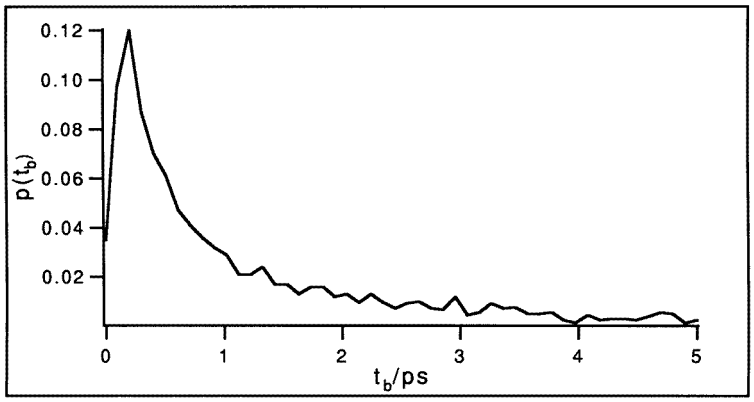

Figure 3. The distribution of bond lifetimes. The mean lifetime is 1.4 ps.

and $p(t)\,\mathrm{d}t$ is the probability that the bond survives a time interval of $[t - \mathrm{d}t/2, t + \mathrm{d}t/2]$. This results in a bond lifetime of $T = 1.3$ ps which corresponds to three to four vibrational periods.

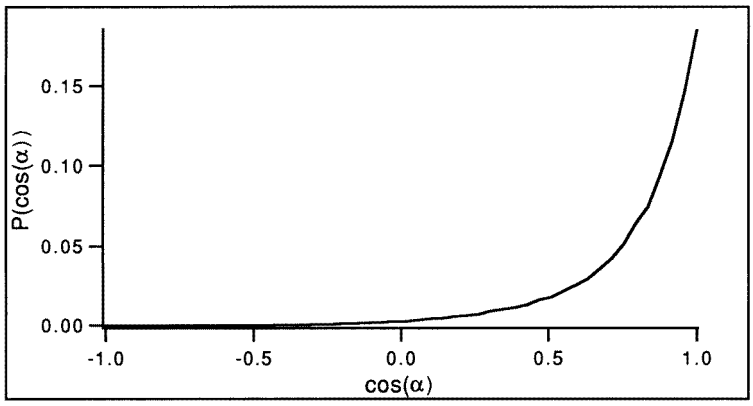

Figure 4. The distribution of the bonding angles between two molecules.

The combination of an effective dipole potential and an isotropic Lennard-Jones potential should result in linear bonding between two molecules. In order to check this conjecture we have examined the distribution of bonding angles and the distribution of distances of the bond forming charges of bonded molecules (figures 4 and 5, respectively). The distribution of the angles displays linear bonding and confirms this idea. A comparison between the distribution for the bonding distances and the first shell of the pair correlation function (figure 6) of opposite charges shows that all bonding distances lie in the first shell. Thus the bonding criterion is appropriate. The little feature after the maximum of the second shell at about 5.45 Å in the pair correlation function is a consequence of the strong linear bonding of the molecules. Its position is just the distance between e.g. the positive charge of a molecule A and the negative charge of a molecule B which is bonded at the negative charge of A. Even though linear bonding is preferred bonding angles around 90° still occur

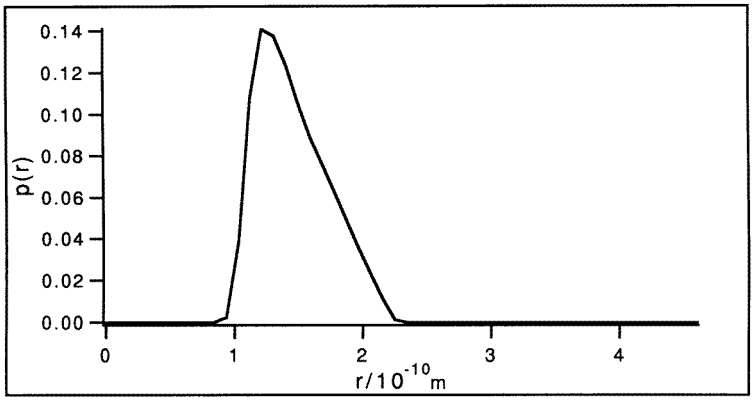

Figure 5. The distribution of the bonding distances. The bonding distance is the distance between the two bond forming charges.

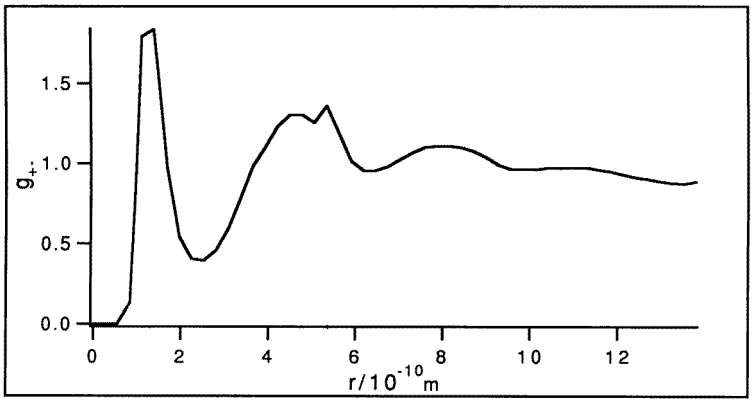

Figure 6. The pair correlation function between opposite charges.

with small probabilities, so one might ask which bonding energies belong to a certain angle. For this reason we have calculated the two-dimensional probability distribution for bonding energies and bonding angles (figure 7). The plot can be interpreted as the probability distributions of bonding energies for a given angle or vice versa. The only change of the angular distribution with rising bonding energies is a concentration at $\cos(\alpha) = 1$ whereas the bonding energy distribution develops an increasing maximum which shifts to larger bonding energies with increasing $\cos(\alpha)$.

It may be noted that linear bonding is the only possible dynamically stable arrangement of two isolated model molecules compared to the case of two formamide molecules, which can be arranged as a cyclic dimer as well [18, 19]. This restricts the compatibility of our model molecule to the formamide molecule but simplifies the task of defining quantities which allow direct insight into the structure of our model liquid.

With the obtained information one can imagine that, similar to methanol with a long winding chain [11, 12] as the typical structure element, our model liquid possesses a more or less straight chain as a typical structure element. This can be verified with a look at the

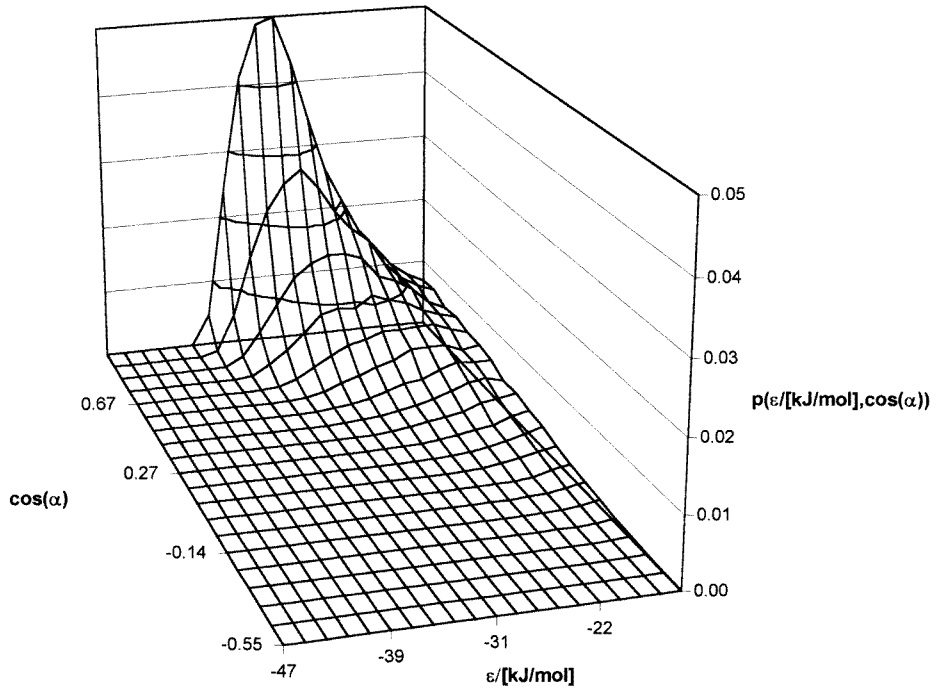

Figure 7. The two-dimensional probability distribution for pair energy and bonding angle.

ensemble in figure 8.

With this picture in mind we have examined the chain size distribution for our liquid layer and distinguished between the bulk part of the liquid and the interfacial part. The regions which we have declared as the bulk part and interfacial part are marked in the density profile in figure 9.

3.2. Chain size distributions

We characterized the chain size by counting the number l of molecules in a chain. We found two meaningful criteria for assigning chains to either surface or bulk regions. One possibility is to compute the number of bulk molecules or surface molecules respectively which are part of a chain with length l. This means that the z dependence of the distributions follows from the location of single molecules. Figure 10 shows the distributions according to this method. The dashed line is the bulk distribution and the full line is the surface distribution. The fact that the two distributions are different furnishes us already with a hint to the orientation of the chains: a mostly perpendicular orientation relative to the surface plane especially of the longer chains would lead to the same distributions for bulk and surface as these chains would contribute to both distributions, so the difference between the two distributions is caused by chains which are completely in the bulk or in the surface region. This points out a parallel orientation of the chains in the surface region. Additional support for this idea is supplied by a second method of z localization. Instead of taking the z coordinate of single molecules one takes the z coordinate of the centre of mass of a chain, so a chain is located in the bulk if its centre of mass is in the bulk and a chain is located in the surface

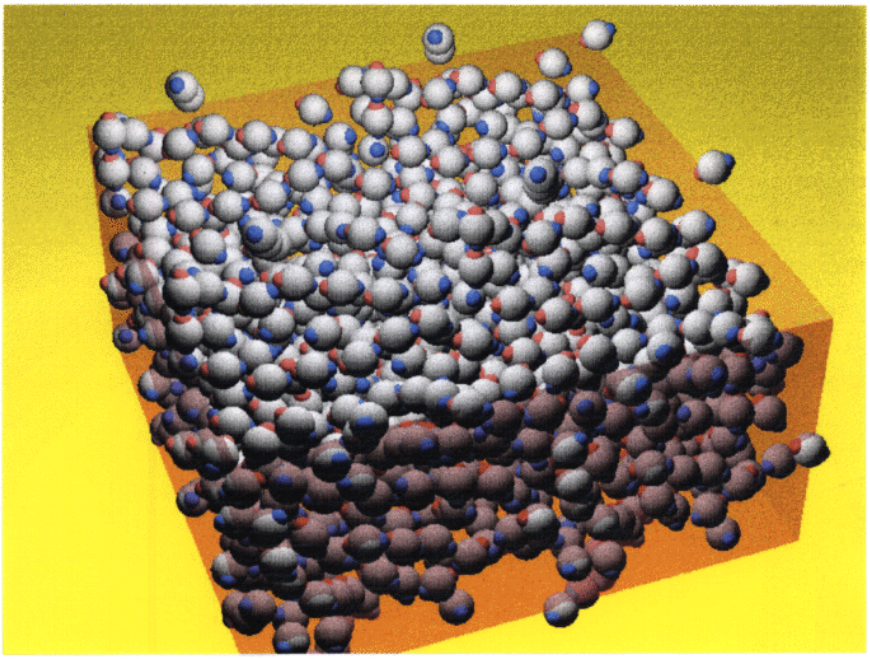

Figure 8. A snapshot of the liquid layer. As some of the chains extend over more than one cell an ensemble of four cells is shown. The outer sites with the negative or positive charges respectively are symbolized with blue or red spheres. The central site is shown as a grey sphere.

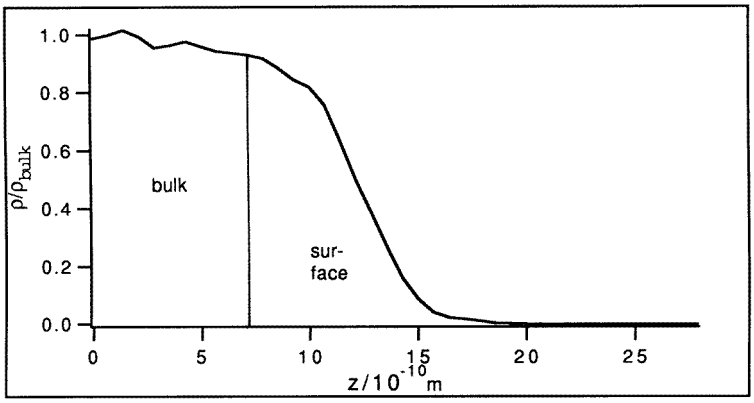

Figure 9. The density profile of the liquid layer. The perpendicular line separates the bulk and the surface parts of the layer.

if its centre of mass is in the surface. We then have calculated the distribution of number of molecules belonging to a bulk chain or surface chain of size l. In figure 10 we also show the results according to the second method of computing the distribution of particles in a chain of length l. The dash–dotted line is the surface distribution and the short-dashed line is the bulk distribution calculated according to the second method. The calculation of the distributions according to the second method leads to a stronger distinction between

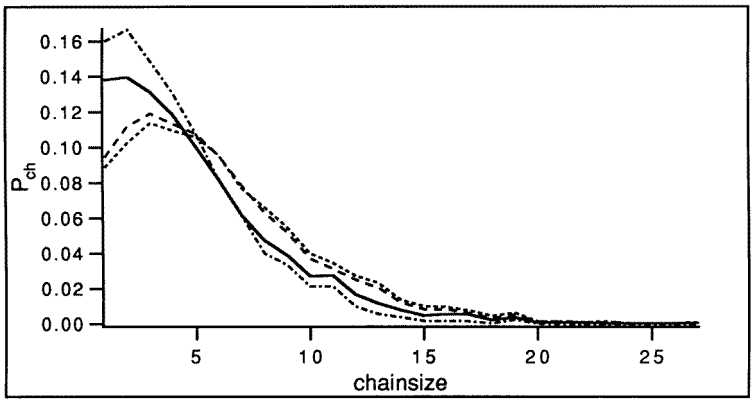

Figure 10. The averaged number of particles belonging to bulk or surface and to a chain of size l calculated according to methods 1 and 2 (see subsection 3.2). Full line, surface distribution, method 1; dashed line, bulk distribution, method 1; dash–dotted line, surface distribution, method 2; short-dashed line, bulk distribution, method 2.

the surface and the bulk. This fact is due to the possibility that in the first method chains may contribute to both distributions whereas in the second method the chains are uniquely assigned to either surface or bulk. However even with the second method a substantial number of molecules in the surface can be found in chains with a length of five or larger. These chains have to be oriented more or less parallel (more with growing chain size) to the surface plane in order to have their centre of mass still in the surface region. This matches the result of a previous simulation with the same molecule [6]. In this simulation it was shown that the individual molecules favour an orientation parallel to the surface plane in the surface region so chains formed by these molecules possess the same orientation.

The feature common to both methods discussed above is a preference for longer chains in the bulk compared to the surface. An explanation may be the higher mobility of molecules in the surface region as already demonstrated in [4] on a Stockmayer fluid. The mobility can be quantified with the aid of the mean squared displacement. Similarly to [4] we have calculated the mean squared displacement perpendicular and parallel to the surface plane and differentiate between bulk and surface regions. Some care has to be taken in the definition and the interpretation of these quantities. Since the bulk region and the surface region are of finite thickness it is possible that a molecule is in one region at time t_k and in the other region at later time t_{k+l}. So there are two possibilities to define the mean squared displacement for a certain region, namely whether one includes molecules which are leaving the actual region in the time interval $t_{k+l} - t_k$ or not. Let $N(z)$ be the average number of molecules in bulk or in the surface region ($z =$ bulk, surface) then one defines

$$d_{\parallel}^2(t_l, z) = \frac{1}{MN(z)} \sum_{k=1}^{M} \sum_{i=1}^{N} ((x_i(t_{k+l}) - x_i(t_k))^2 + (y_i(t_{k+l}) - y_i(t_k))^2) I(z_i(t_{k+l}), z_i(t_k), z)$$

$$d_{\perp}^2(t_l, z) = \frac{2}{MN(z)} \sum_{k=1}^{M} \sum_{i=1}^{N} ((z_i(t_{k+l}) - z_i(t_k))^2 I(z_i(t_{k+l}), z_i(t_k), z)$$

$$I(z_i(t_2), z_i(t_1), z) = \delta(z_i(t_1), z) \tag{1}$$

$$I(z_i(t_2), z_i(t_1), z) = \delta(z_i(t_1), z)\delta(z_i(t_2), z) \tag{2}$$

$$\delta(z(t), z) = 1 \Leftarrow z(t) \in z \qquad \delta(z(t), z) = 0 \Leftarrow z(t) \notin z \qquad z = \text{bulk, surface.}$$

The calculation of the mean squared displacement using equation (1) does not take into account whether a molecule is leaving the region during the observed time interval (method 1), whereas using equation (2) results in taking into account only those molecules which are in the region at the beginning and at the end of the observed time interval (method 2).

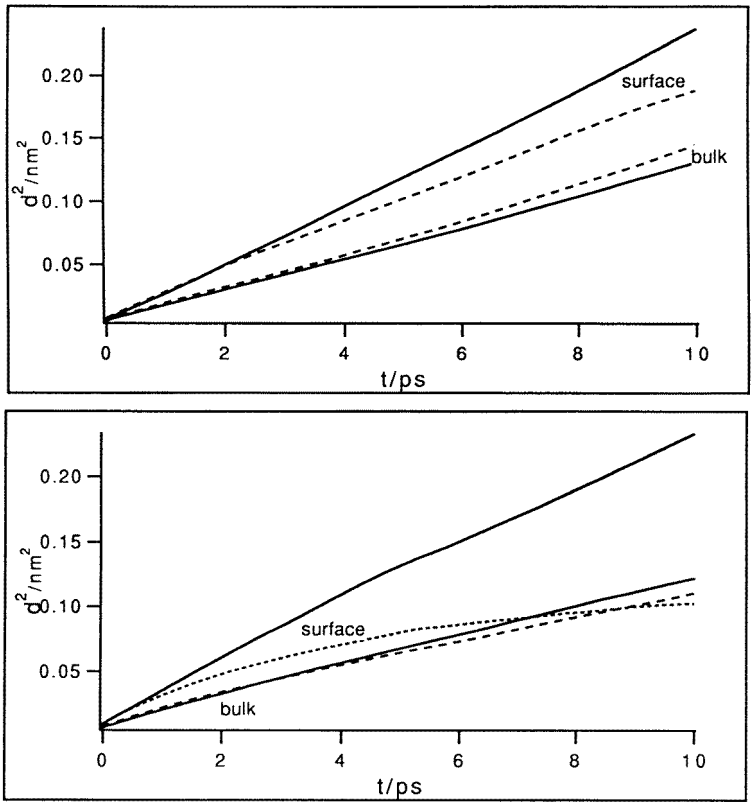

Figure 11. Mean squared displacements of molecules in the liquid layer. The upper panel shows the mean squared displacements calculated with method 1; the lower panel corresponds to method 2. The dashed lines are displacements perpendicular to the surface plane and the full lines are the mean displacements parallel to the surface plane.

Figure 11 displays the mean squared displacement of the molecules in the bulk and the interfacial regions calculated according to method 1 (upper panel) and method 2 (lower panel). The dashed lines are the mean squared displacements perpendicular to the surface and the straight lines are the mean squared displacements parallel to the surface. We find a general enhanced displacement in the surface region together with an increased mobility parallel to the surface plane compared to the mobility perpendicular to the surface plane. This indicates anisotropic dynamics in this region. The net result is an increased mobility in the surface region. In addition to that we observe a remarkable difference between methods 1 and 2 in the estimation of the mobility in the surface region in the direction perpendicular to the surface plane. The calculation with method 1 yields a nearly straight line whereas method 2 results in a curve with an upper limit. This is due to the fact that in method 2 molecules are taken into account only if they are not diffusing back into the bulk region. The only possibility to achieve an unlimited rise would be the evaporation of

most of the surface molecules into the vapour or vacuum since these regions are included in our definition of the surface region, so the existence of an upper limit of the mean squared displacement perpendicular to the surface plane in the surface region indicates the stability of the surface layer. Further, one has to state that generally the evaporation of a molecule is an extremely unlikely event on the time scale of an MD calculation which is below 10^{-9} s. For comparison, the evaporation of one monolayer of water at room temperature requires several microseconds.

3.3. Topological correlation between chains

Next we want to analyse the topological correlation between chains. In this respect only chains which are somehow close to each other can be of interest, so we have to define a distance between two chains. This distance is taken to be the minimum of the pairwise distances between the central sites of two molecules of the chains inspected. With this distance we calculated a pair correlation function for chains in order to obtain a quantitative criterion to decide whether a chain is a neighbour of another chain or not (figure 12). The normalization procedure is the same as for a site–site correlation function. The pair correlation function shows a pronounced first shell and a smaller second shell. Only chains whose distances are smaller than the minimum between the first and the second shell are considered as neighbours.

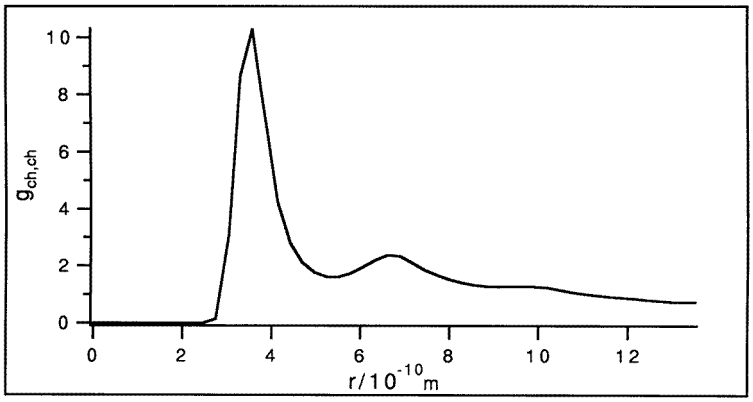

Figure 12. The pair correlation function of the distance between chains. This distance is defined as the distance between the central sites of the two molecules which are closest.

An interaction between chains may lead to a preferred geometrical arrangement between chains. To check this proposition we have examined the angles between the dipoles which belong to those molecules of the neighbouring chains which are closest. These molecules will be called the distance pair for short in the following and the corresponding angle the distance pair angle. As a second possibility we also have examined the angles between the dipoles which belong to those molecules of the neighbouring chains which have the lowest pair energy. These molecules will be called the energy pair for short in the following and the corresponding angle the energy pair angle. We have focused on these two possibilities as the interaction between the chains can be expected to be strongest at these particular points. This analysis is further split depending on the length of the participating chains. Figure 13 shows the distribution of $\cos(\theta)$ with θ being the distance pair angle if the minimum length of the

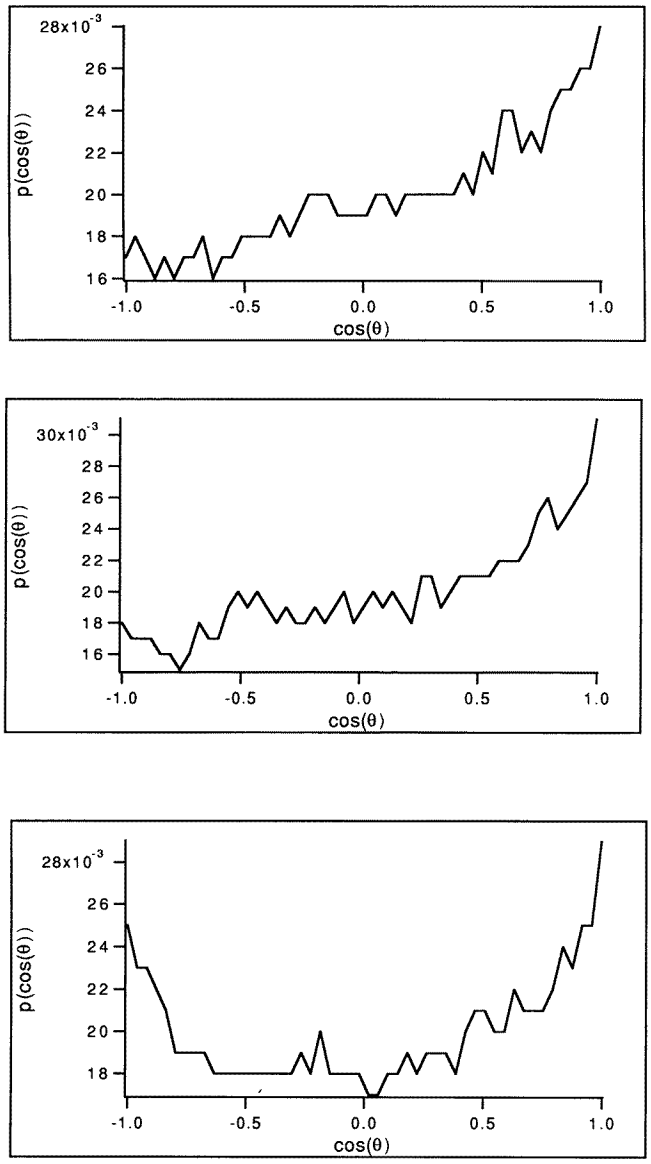

Figure 13. The distribution of $\cos(\theta)$. θ is the angle between the two closest molecules of two neighbouring chains. The plots are the distribution if the minimum length of the participating chains is equal to two, equal to three and equal to four or larger (from top to bottom).

participating chains is equal to two, equal to three and equal to four and larger (from top to bottom). Of course this distinction is somewhat arbitrary but a more systematic investigation would require much longer runs. All the same, some effects seem to be above statistics. The distributions indicate that for neighbouring chains with a shorter chain ($l = 2$ or $l = 3$) taking on a parallel arrangement of the dipoles is preferred. In figure 14 two situations are displayed which can be understood as parallel or antiparallel orientation. If the neighbouring

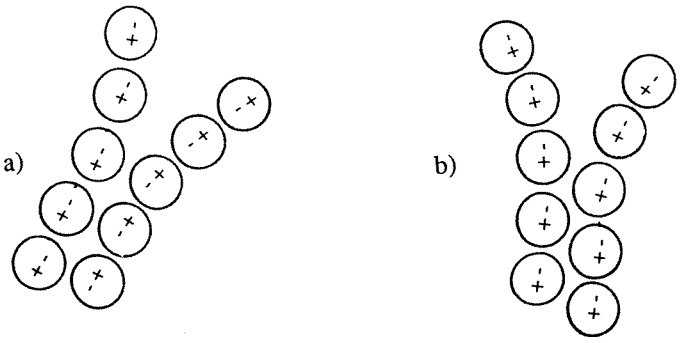

Figure 14. (a) The possibility of antiparallel arrangement between molecules of neighbouring chains; (b) the possibility of parallel arrangement between molecules of neighbouring chains.

chains have a minimum length of four or larger a substantial number of the correlated dipoles are orientated antiparallel. This indicates that this way of orientation is stabilized with increasing chain size of the neighbouring chains, but still the parallel arrangement is slightly preferred. In figure 15 the $\cos(\theta)$ distributions are shown with θ being the energy pair angle. The dotted line is the distribution for pairs of chains with minimum length equal to two, the dashed line for minimum length equal to three and the full line is the distribution for minimum length of four and more. Again one can observe a pronounced tendency for antiparallel orientation with increasing minimum chain length. In contrast to the distributions calculated with the two closest molecules (figure 13), the parallel arrangement is suppressed. A possible conclusion is that the antiparallel orientation between molecules of neighbouring chains leads to a lower pair energy than the parallel orientation. The distribution of the pair energies of molecules with a 'bonding angle' larger than 100° (figure 16) reveals that even though the energies are below zero, they are still well above those of the usual bonding (figure 1). This result together with the above proposed possible conclusion (the antiparallel orientation between molecules of the two neighbouring chains yields a lower pair energy than the parallel one) indicates that the parallel arrangement of molecules between neighbouring chains is of quite a different nature than the usual bonding. The lifetime distribution of the antiparallel bonding is shown in figure 17. The resulting mean lifetime is 0.7 ps.

3.4. Parameter variation

3.4.1. Variation of the moment of inertia. To analyse the influence of the moment of inertia on the discussed quantities we repeated the simulation with a modified mass distribution. In contrast to the former model molecule with the mass equally distributed on the outer sites and no mass on the central site, the mass is now concentrated on the central site. Let m_c be the mass of the central site and m_0 the mass of one of the outer sites, then $m_c = 8m_0$ and $2m_0 + m_c = m$ with m as given in table 1.

In figure 18 the distributions of numbers of bulk molecules or surface molecules which are part of a chain with length l (method 1) are displayed. Again there is a preference for larger chains in the bulk than in the surface region. This can be explained by the same behaviour of the mobility as observed before (see figure 11).

A difference from the molecule with the masses on the outer sites occurs in the distribution of $\cos(\theta)$ with θ being the distance pair angle (figure 19). The dashed line is the

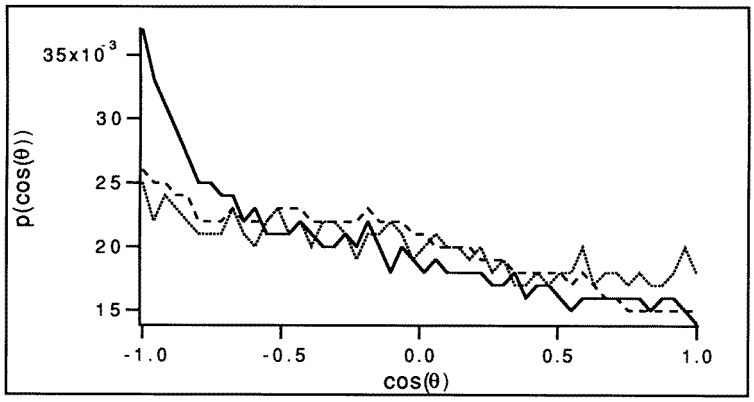

Figure 15. The distribution of $\cos(\theta)$. θ is the angle between the two molecules with the lowest pair energy of two neighbouring chains. The dotted line is the distribution for pairs of chains with minimum length equal to two, the dashed line for minimum length equal to three and the full line is the distribution for minimum length equal to four or more.

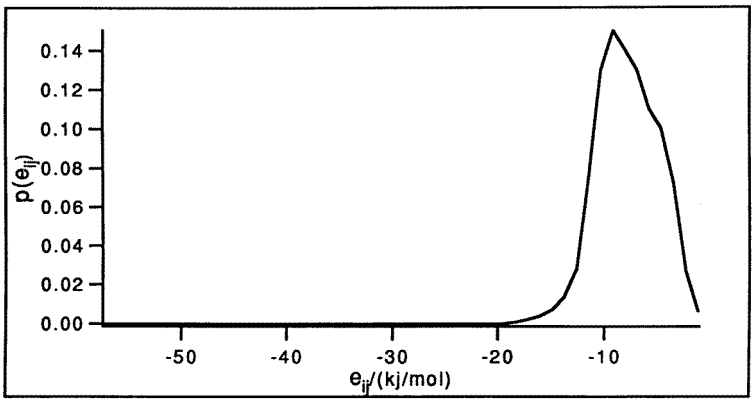

Figure 16. The distribution of pair energies between molecules with a bonding angle bigger than 100°.

angle distribution if the minimum chain size is equal to two; the full line is the distribution if the minimum chain size is equal to four or larger. The parallel arrangement is preferred in all three inspected situations, namely if the minimum length of the participating chains is equal to two, equal to three or four and larger (only the distributions for minimum chain size two or four and larger are displayed; the distribution with minimum chain size equal to three lies between the two shown distributions but is omitted). There is only a spurious rise of the antiparallel arrangement with increasing minimum chain size. The reason may be that the antiparallel arrangement loses stability due to an increase in the amplitude of the rotational vibration caused by the lighter outer sites. This also corresponds to the distribution of the bond lifetime (figure 20) of the antiparallel bonding which leads to a shorter mean lifetime as before, 0.45 ps, and which shows bigger probabilities of the short lifetimes. If we examine the distributions of $\cos(\theta)$ with θ being the energy pair angle we obtain a similar distribution as before but with smaller differences between the angle distributions with minimum chain

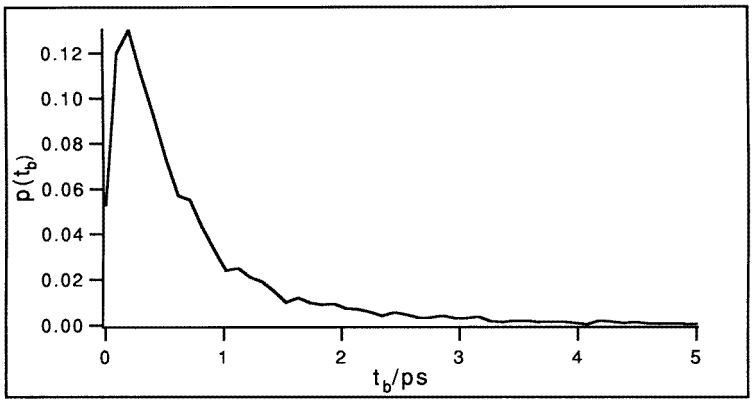

Figure 17. The lifetime distribution of 'bonded' molecules with a bonding angle bigger than 100°.

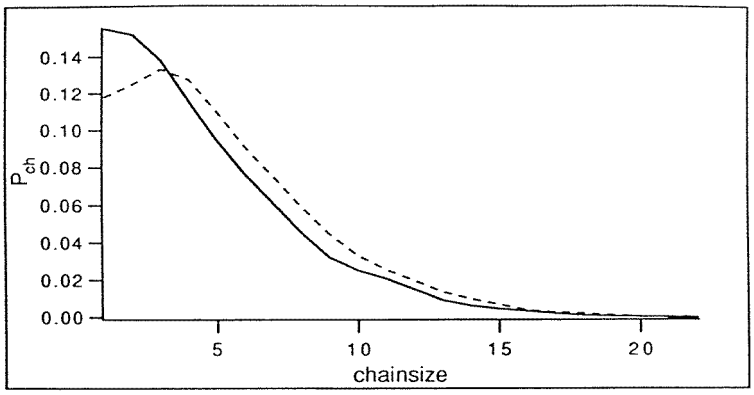

Figure 18. The distribution of the averaged number of molecules which belong to bulk or surface and are part of a chain of length l (method 1) The full line is the surface distribution and the dotted line is the bulk distribution. Results are obtained with the modified mass distribution.

size equal to two and four (figure 19; the dotted line corresponds to minimum chain size equal to two and the dashed–dotted line to minimum chain size equal to four or larger).

3.4.2. Variation of the dipole moment. At the beginning of this study we used higher partial charges than the ones given in table 1 namely $q = \pm 0.16\ e$. The masses were on the outer sites. This choice of parameters resulted in a mean chain size larger than the box length, which means that the chosen magnitude of the partial charges was too large for the system size. Nonetheless we observed remarkable effects with regard to the correlation between the chains. The distributions of $\cos(\theta)$, with θ being the distance pair angle, are displayed in figure 21. Again the distributions are split according to the minimum length of the participating chains. The short-dashed line is the distribution for minimum length equal to two, the dashed line for minimum length equal to three and the full line for minimum length four and larger. Again, the probability of the antiparallel arrangement is increased with increasing chain size. In figure 22 we compare the distributions for minimum length

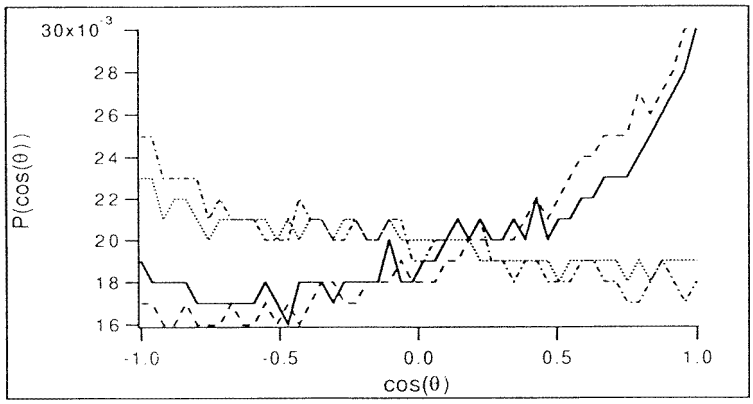

Figure 19. The distribution of $\cos(\theta)$. θ is the angle between the two closest molecules of two neighbouring chains or the angle between the two molecules with the lowest pair energy. The dashed line is the distribution of $\cos(\theta)$ with θ being the angle between the two closest molecules if the minimum chain size is equal to two; the full line is the distribution if the minimum chain size is four or larger. The dotted line is the distribution of $\cos(\theta)$ with θ being the angle between the two molecules with the lowest pair energy if the minimum chain size is equal to two; the dashed–dotted line is the distribution if the minimum chain size is equal to four or larger. Results are obtained with the modified mass distribution.

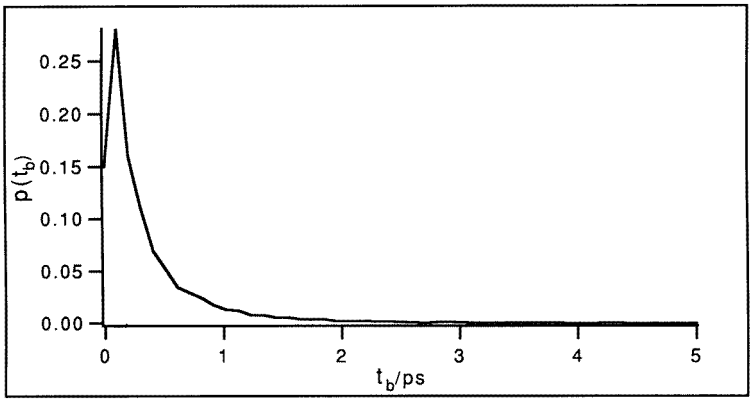

Figure 20. The distribution of the bond lifetime of the antiparallel bonding obtained with the modified mass distribution.

four and larger resulting from the low and higher dipole moments. One can see the enhanced interaction of chains in the system with the higher dipole moment, but as shown in figure 14 the system with the lower dipole moment still displays a similar behaviour.

4. Summary

We have simulated a liquid layer consisting of quasi-Stockmayer molecules. Graphical illustration of the ensemble shows that the molecules form chains. The bonding between two molecules has been explored to support the impression of linear or slightly curved chains

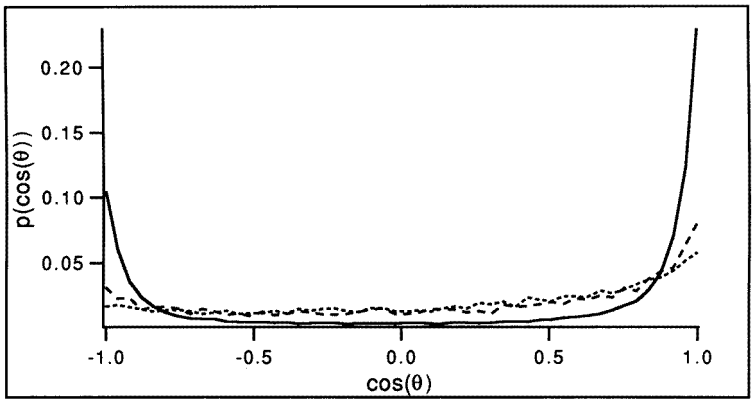

Figure 21. The distribution of $\cos(\theta)$. θ is the angle between the two closest molecules of two neighbouring chains. The short-dashed line is the distribution if the minimum length of the participating chains is equal to two, the dashed line if the minimum length is equal to three and the full line if the minimum length is four or larger. This plot resulted from a simulation with partial charges increased from $q = 1.3609\ e$ to $q = 1.6\ e$.

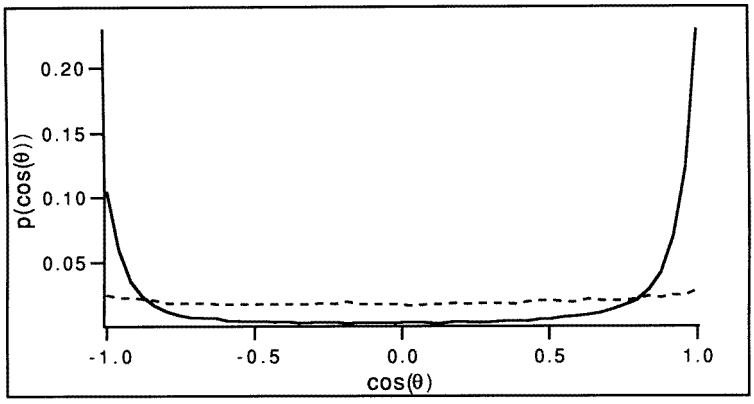

Figure 22. A comparison of the distribution of $\cos(\theta)$ resulting from the simulation with partial charges $q = 1.3609\ e$ and $q = 1.6\ e$. θ is the angle between the two closest molecules of two neighbouring chains. Displayed are the distributions for chain lengths equal to four or larger.

and to obtain a bonding criterion. We have calculated the chain size distribution for the bulk part and the surface of the layer and found that in the bulk part of the liquid longer chains are more likely to occur. This has been explained by the higher mobility of the molecules in the surface region which lowers the probability of bond formation. Furthermore, we have investigated orientational arrangement between the chains themselves. We have examined in detail the angles between those molecules of two neighbouring chains which are closest or between those with the lowest pair energy. We have subdivided this examination depending on the length of the smaller chain. It appears that there is a slight preference that the two closest molecules of the neighbouring chains align their dipoles. If the chain sizes of the two participating chains are larger than three an increase in the probability that the two closest molecules antialign their dipoles can also be observed. The larger the chain

size the more prefer neighbouring chains to align or antialign the dipoles of their closest molecules. The comparison of the two possibilities for calculating the angle distribution (angle between the two closest molecules or between the two molecules with the lowest pair energy) indicates that the pair energy of the antiparallel arrangement between two molecules of the neighbouring chains is lower than that of the parallel arrangement. The pair energy distribution of the antialigned molecules has revealed that these energies are above the respective values of the usual bonding, so one can conclude that the parallel arrangement between the dipoles of the two closest molecules is different from the usual bonding.

A change of the mass distribution to a smaller moment of inertia yields a decrease in the probability of antialigning the neighbouring dipoles. A possible reason is the loss of stability of the antiparallel arrangement due to an increased amplitude of the rotational vibration caused by the lighter outer atoms. However, the parallel arrangement is still a preferred orientation between the correlated dipoles.

Our system shows two levels of structure formation: The building of chains by bonded molecules and the arrangement of chains in preferred orientation.

Acknowledgments

The authors would like to thank J Oberbrodhage for help on figure 8. JD is also grateful for stimulating discussions with collaborators of A Geiger's group in Dortmund. In addition to this we thank the Scientific Council of the Höchstleistungsrechenzentrum at the Forschungs Zentrum Jülich for generous allotment of computer time on the Cray Y-MP/832. The Deutsche Forschungs Gemeinschaft is gratefully acknowledged for financial support.

References

[1] Rowlison J S and Widom B 1982 *Molecular Theory of Capillarity* (Oxford: Clarendon)
[2] Thompson S M and Gubbins K E 1981 *J. Chem. Phys.* **74** 6467
[3] Thompson S M 1978 *Faraday Discuss.* **66** 107
[4] Eggebrecht J, Thompson S M and Gubbins K E 1986 *J. Chem. Phys.* **86** 2299
[5] Eggebrecht J, Gubbins K E and Thompson S M 1986 *J. Chem. Phys.* **86** 2286
[6] Hertzner A W, Schoen M and Morgner H 1991 *Mol. Phys.* **73** 1011–29
[7] Matsumoto M and Kataoka Y 1988 *J. Chem. Phys.* **88** 3233
[8] Matsumoto M and Kataoka Y 1989 *J. Chem. Phys.* **90** 2398
[9] Amaral L A N and Cabral B J C 1993 *J. Phys.: Condens. Matter* **5** 1919–34
[10] Rahman A and Stillinger F H 1973 *J. Am. Chem. Soc.* **95** 7943–8
[11] Mausbach P, Schnitker J and Geiger A 1987 *J. Tech. Phys.* **28** 67–76
[12] Jorgensen W L 1986 *J. Phys. Chem.* **90** 1276
[13] Haughney M, Ferrario M and McDonald I R 1987 *J. Chem. Phys.* **91** 4934
[14] Matsumoto M and Gubbins K E 1990 *J. Phys. Chem.* **93** 1981
[15] Siegbahn H, Asplund L, Kelfve P, Hamrin K, Karlson L and Siegbahn K 1974 *J. Electron. Spectrosc. Relat. Phenom.* **5** 1059
[16] Hippler M and Hertz H G 1992 *Z. Phys. Chem.* **175** 25
[17] Jorgensen W L and Swenson C J 1985 *J. Am. Chem. Soc.* **107** 569
[18] Puhovski Y P and Rode B M 1995 *Chem. Phys.* **190** 61–82
[19] Schoester P C, Zeidler M D, Tamas Radnai and Bopp P A 1995 *Z. Naturf.* a **50** 38–50
[20] Bitsanis I and Ionnis A 1993 *J. Chem. Phys.* **99** 5520–7
[21] Bitsanis I and Hadziionnou G 1990 *J. Chem. Phys.* **92** 3827–47
[22] Rybarsky M W and Landman U 1992 *J. Chem. Phys.* **97** 1937–49
[23] Smith W *CCP5 Newslett.* **7** 5
[24] Alejandre J, Tildesley D J and Chapela G A 1995 *J. Chem. Phys.* **102** 4574
[25] Eisenberg D and Kauzman W 1969 *The Structure and Properties of Water* (London: Clarendon)